Aalto University
School of Science

Master's Programme in Mathematics and Operations Research

An extension of the Black-Scholes-Merton options pricing model to Ethereum

Teemu Laurikainen

Master's Thesis
2025

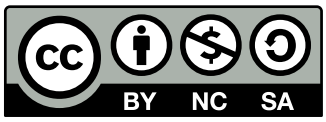

Aalto University
School of Science

Author Teemu Laurikainen

Title An extension of the Black-Scholes-Merton options pricing model to Ethereum

Degree programme Mathematics and Operations Research

Major Applied Mathematics

Supervisor Prof. Ahti Salo

Advisor D.Sc. (Tech.) Ruth Kaila

Collaborative partner -

Date 28th January 2025 **Number of pages** 56 **Language** English

Abstract

Ethereum is the second largest crypto protocol in the world in terms of market capitalization and the size of the user and developer community.

Ether (ETH), the native token of the protocol, has unique characteristics as a financial asset but resembles a combination of a currency, a commodity, and a security. At the time of writing, the total market capitalization of ETH is $381 billion.

This thesis proposes a novel approach to incorporate the dynamics of supply changes in the valuation of ETH call options. Mathematically, a modified Black-Scholes-Merton (BSM) options pricing model is formulated for ETH. A comparison analysis is performed with synthetic data and historical market data from Deribit, the largest exchange of ETH options by volume. In addition, implied volatilities are estimated using the approach.

The numerical results confirm the theoretical behavior of the volatility structures with the addition of supply dynamics to the BSM model. In particular, volatility structures experience an increasing skewness for deep-in-the-money call options.

Keywords Ethereum, options, options pricing models, implied volatility

Aalto-yliopisto
Perustieteiden
korkeakoulu

Tekijä Teemu Laurikainen

Työn nimi Black-Scholes-Merton-mallin soveltaminen Ethereumille

Koulutusohjelma Matematiikka ja operaatiotutkimus

Pääaine Sovellettu matematiikka

Työn valvoja Prof. Ahti Salo

Työn ohjaaja TkT Ruth Kaila

Yhteistyötaho -

Päivämäärä 28.01.2025 **Sivumäärä** 56 **Kieli** englanti

Tiivistelmä

Ethereum on maailman toiseksi suurin kryptoprotokolla markkina-arvon ja käyttäjämäärän suhteen.

Ether (ETH), protokollan oma virtuaalivaluutta, omaa uniikkeja ominaisuuksia rahoitusvälineenä, mutta muistuttaa yhdistelmää valuutasta, hyödykkeestä ja arvopaperista. ETH:n kokonaismarkkina-arvo on 381 miljardia dollaria.

Diplomityössä ehdotetaan uutta lähestymistapaa Ethereum-optioiden arvostukseen, joka ottaa huomioon kokonaistarjonnan muutosdynamiikan. Matemaattisesti Black-Scholes-Merton (BSM) optiohinnoittelumallia muokataan ETH:lle sopivaksi. Vertailuanalyysi suoritetaan käyttäen synteettistä dataa, sekä historiallista markkinadataa Deribit-pörssistä, joka on volyymiltaan suurin ETH-optioiden pörssi. Lisäksi arvioituja implisiittisiä volatiliteetteja lasketaan uutta lähestymistapaa käyttäen.

Numeeriset tulokset vahvistavat mallin teoreettisten volatiliteettirakenteiden käyttäytymisen. Erityisesti volatiliteettirakenteet kokevat kasvavaa vinoumaa voimakkaasti voitolla oleville osto-optioille.

Avainsanat Ethereum, optiot, optioiden hinnoittelumallit, implisiittinen volatiliteetti

Preface

The book of nature is written in the language of mathematics.

— Galileo Galilei, 1623

Otaniemi, 28th January 2025

Teemu Laurikainen

Acknowledgements

I would like to extend my gratitude to my advisor, D.Sc. (Tech.) Ruth Kaila, for her remarkable depth of understanding in the field of quantitative finance, and to my supervisor, professor Ahti Salo, for his excellent academic guidance. To my family, thank you for your everlasting support.

Contents

Abstract 3

Abstract (in Finnish) 4

Preface 5

Acknowledgements 6

Contents 7

Symbols, acronyms and abbreviations 9

1 Introduction 12
- 1.1 Background . . . 12
- 1.2 Research objectives and questions . . . 13
- 1.3 Structure of the thesis . . . 13

2 Ethereum 14
- 2.1 Ethereum protocol . . . 14
- 2.2 Ethereum token (ETH) and supply dynamics . . . 15
- 2.3 ETH as a financial asset . . . 17
- 2.4 Derivative and option markets for ETH . . . 18
- 2.5 Ethereum options literature . . . 19

3 Options 20
- 3.1 Stochastic calculus . . . 20
  - 3.1.1 Probability theory . . . 20
  - 3.1.2 Stochastic processes . . . 21
  - 3.1.3 Brownian motion . . . 22
  - 3.1.4 Itô's calculus . . . 23
- 3.2 Option pricing . . . 24
  - 3.2.1 Black-Scholes in differential form . . . 24
  - 3.2.2 Black-Scholes closed solutions . . . 25
  - 3.2.3 Merton dividends adjustment and BSM . . . 26

4 Research methods 29
- 4.1 Modified BSM for Ethereum options . . . 29
  - 4.1.1 Mathematical formulation . . . 29
  - 4.1.2 Crypto asset BSM . . . 32
  - 4.1.3 Model assumptions . . . 33
- 4.2 Data acquisition . . . 37
  - 4.2.1 Synthetic data . . . 37
  - 4.2.2 Deribit options exchange . . . 38
- 4.3 Analysis overview . . . 39

4.3.1 Numerical methods 39

5 Results and analysis **41**
5.1 Model comparison with synthetic data 41
5.2 Model comparison with Deribit data 46
5.3 Key findings 49

6 Conclusions **50**
6.1 Discussion 50

Symbols, acronyms and abbreviations

Symbols

$\mathbb{E}[\cdot]$	Expectation
$\mathbb{V}ar[\cdot]$	Variance
dt	Infinitesimally small time increment
S_t	Stock price at time t
μ	Expected return
σ	Volatility of the stock's returns
B_t	Brownian motion at time t
r	Risk-free rate
K	Strike price of the option
T	Maturity of the option
$C(t, S_t)$	Price of a European call option at time t with stock price S_t
$\mathcal{LN}$	Lognormal distribution
Π	Portfolio
q	Continuous dividend yield

Acronyms and Abbreviations

Term	Definition
Ethereum	A blockchain-based protocol for decentralized applications
ETH	Ether or Ethereum token, the virtual currency native to the Ethereum protocol
HTTP, IP, DNS	Communications protocols used on the Internet.
EVM	Ethereum Virtual Machine
EIP	Ethereum Improvement Proposal
Blockchain	A distributed ledger technology that allows data to be stored across a network of computers.
Proof-of-stake	A type of algorithm by which a blockchain protocol aims to achieve distributed consensus.
Proof-of-work	A type of consensus algorithm that relies on competition of computational effort.
Slashing	Punishment for a validator's malicious behaviors in proof-of-stake blockchain systems
Smart contract	Self-executing program code on blockchain protocols
Staking	Holding and locking cryptocurrencies in an account to support operations such as transaction validation and network security in proof-of-stake blockchains.
Gas	A measure of computational effort in Ethereum, denoting the cost to perform transactions or smart contract interactions.
Dapps	Decentralised applications that run on a blockchain protocol.
Spot trading	The buying or selling of a financial instrument for immediate delivery and payment.
BSM model	Black-Scholes-Merton options pricing model, a group of mathematical formulas to value options where the underlying is a stock. Often used to derive implied volatilities from option prices.
European call option	An option contract that gives the holder the right, but not the obligation, to buy the underlying asset at a specified price on a specific date.
Implied volatility	The volatility derived from the actual market value of an option often using the BSM model.
Volatility smile	A pattern in which at-the-money options tend to have lower implied volatilities than in- or out-of-the-money options.

1 Introduction

1.1 Background

Ethereum is a global computing platform on top of which anyone is open to build decentralized applications [1]. The system is fundamentally at the intersection of various fields, including finance, computer science, mathematics, and politics. Therefore, the system can be defined from various perspectives. This thesis focuses mostly on the financial aspects of Ethereum and, in particular, on the option market dynamics of the crypto asset Ether (ETH).

The thesis is motivated by the nascent nature of the crypto industry and the lack of existing research on options pricing models for crypto assets. Existing option pricing models have been fine-tuned for traditional asset classes, such as stocks, futures, and foreign currencies. However, crypto assets are a completely new asset class and option pricing models have to be considered together with their unique characteristics and adjusted if necessary. If the total crypto asset market capitalization continues to increase, as historically it has, these pricing model adjustments become increasingly important in the context of pricing accuracy and market efficiency. Extensions to specific crypto assets such as ETH are not widely found in the literature.

Considering ETH in the context of the Black-Scholes-Merton option pricing model, now known as the "BSM" model, it can be applied directly with the assumption that ETH is a non-dividend paying stock [2]. However, ETH resembles a combination of a currency, a stock, and a commodity, as will be discussed in detail later in the thesis. ETH is not a plain stock. ETH is a non-dividend paying crypto asset with a dynamic supply change parameter.

Critically, the BSM model does not directly capture the supply-change dynamics of ETH, which should have an obvious effect on option valuations. As an example, if we consider an annual supply change of 10% of the underlying until perpetuity, then we should expect the underlying to be diluted by some percentage of value annually. Taking a comparison from traditional finance, mathematically, a stock split does not result in the creation of additional value. This statement can be surprisingly counterintuitive to market participants, as research shows how the market reacts often positively to stock splits [3]. If stock splits systematically created additional value for shareholders, the correct strategy for every existing company in the world would be to immediately attempt to reach infinity with their amount of outstanding shares. In general, corporate actions do not correspond to this strategy.

This comparison is important because it forms the basis for the premise that increasing the amount of shares in a company only results in a dilution of existing shares and no additional value is created. Applied to ETH, if the supply change is positive, existing ETH holders are diluted. Conversely, if the supply change is negative, the value is transferred indirectly to existing ETH holders.

We arrive at the central topic of the thesis; how to incorporate the ETH supply change dynamics into the BSM model? Dividends are just one known form of share value dilution in the BSM model. Is there something in the construction of the BSM model that strictly forces the use of dividends, or can we extend this dilution factor to other mechanisms, such as supply changes? If we can, what about negative supply changes if burn exceeds issuance in the Ethereum protocol?

1.2 Research objectives and questions

The objective of the thesis is to devise a method to assess the applicability of the BSM model to ETH options. This thesis will specifically aim to answer the research questions presented below.

- What impact do supply changes have on the BSM model when pricing ETH options?
- How does the extended BSM model affect option pricing and implied volatility structures compared to the traditional approach?

The scope of the thesis is limited to the consideration of the crypto asset ETH. Although the results of this thesis may be useful for the valuation of other crypto asset options, this study will not focus on any other crypto assets. Furthermore, only the Black-Scholes-Merton model is considered, although numerous option pricing models exist in the financial literature. These models include Heston and Bachelier among others [4] [5]. A key reason for the selection of the BSM model for this study is its widespread use in financial markets and also its mathematical simplicity compared to other models.

In the BSM model, the focus is on the dividend term q, both mathematically and empirically. The scope of the study includes rigorous reasoning on why or why not the definition of the term can be extended to consider other dilution mechanisms in addition to dividends. In addition, an empirical analysis based on options market data is included in the study.

1.3 Structure of the thesis

The thesis continues to Section 2 with an overview of Ethereum. Section 3 presents the mathematical background necessary to have the correct tools to approach the research questions. In Section 4, Research methods, a mathematical formulation of a modified version of the BSM for ETH options is presented, followed by an explanation of how empirical analysis with the options market data from Deribit is conducted. Section 5 presents the results of the analysis. Lastly, Section 6 discusses the results in connection with the original research goals and objectives and summarizes the contents of the thesis.

2 Ethereum

2.1 Ethereum protocol

From a computer science perspective, Ethereum is a protocol on the Internet. In networking, a protocol is a set of rules or processes for transmitting data between electronic devices, such as computers [6]. The most well-known protocols include HTTP, IP, DNS, and other major Internet communications protocols. Ethereum and other crypto-economic systems can be contextually thought of as value transfer protocols. Instead of communications data, the protocol is able to transfer economic value.

Technically, Ethereum is a deterministic and unbounded state machine, consisting of a singleton state that is globally accessible and a virtual machine that changes that state [7]. Alternatively defined, Ethereum is a blockchain; a decentralised peer-to-peer network that leverages cryptography to securely host applications, store data, and transfer digital objects [8]. Instead of simple tracking of currency ownership, Ethereum blockchain tracks the state transitions of a general-purpose data store [7]. Ethereum has an average block-time of approximately 12 seconds, that is, how often a new block is added to the chain [9].

The Ethereum protocol was initially conceptualized in 2013 by Vitalik Buterin in his whitepaper. Motivation for the design of such system arose from Bitcoin's inherent technical limitations, namely, in the difficulty of building and running application code directly on top of Bitcoin. Ethereum's design pioneered the use of smart contracts, program code which is executed trustlessly on the Ethereum blockchain. These contracts are mainly written in Ethereum's native programming language, Solidity. In his paper, Vitalik describes how the Bitcoin protocol facilitates a weak version the concept of smart contracts, but lists serveral technical limitations in Bitcoin's scripting language that makes the use of these contracts practically difficult, notably lack of Turing-completeness [1]. Turing-completeness is important because Ethereum can function as a general-purpose computing platform, often described as a "world computer" [10].

The ability to run and execute smart contract logic on Ethereum opened an unbounded design environment to create and build decentralised applications [10]. Trustless applications are important in the context of the entire decentralized programming paradigm, since they enable protocol logic to be extended from simple value transfer to more complicated financial processes, such as lending, stablecoins, exchanges, or tokenisation of real world assets. As of the time of writing this thesis, the total market capitalisation of all decentralised finance applications is approximately $ 40 billion [11].

2.2 Ethereum token (ETH) and supply dynamics

Ether, or more commonly abbreviated as ETH, is the native crypto currency of the Ethereum protocol, which serves multiple purposes [1]. First, it is used to pay for transaction fees in the Ethereum protocol. Whenever a transaction is sent, the sender incurs a fee in the form of ETH.

These transaction fees are also referred to as "gas" or "fuel" in the Ethereum protocol. The gas system in Ethereum is essentially a metering system to prevent infinite loops from occurring, which are possible in Turing-complete systems. If a party could run a code infinitely, they could consume infinite computing resources from the Ethereum protocol. When the Ethereum virtual machine (EVM) executes a smart contract, it counts the number of instructions in the given code. Each of these instructions has a predetermined cost in units of gas. Before the smart contract code is executed, the sender has to choose the maximum level of gas they are willing to spend. If the computation exceeds this limit, the code will stop running, preventing infinite loops in the system. Fundamentally, the gas system is needed because we cannot predict a path of a program without running it, i.e. the Halting Problem is undecidable as Alan Turing proved in 1936 [12]. Conceptually, the gas system allows a market for computation [13]. [7]

Secondly, Ether is needed as a cryptoeconomic security mechanism to pay the validators to secure transactions and the blockchain consensus [13]. Since September 15, 2022, the Ethereum protocol has operated on a "proof-of-stake" consensus model. This event is called the "Merge". In a proof-of-stake model, validators are responsible for "staking" their capital in the form on Ether and checking the validity of the new blocks that are proposed in the network. Moreover, validators are occasionally responsible for creating and propagating new blocks themselves. The staking mechanism incentivizes honest behavior in consensus systems, because dishonest behavior results in "slashing" of the validators' capital (i.e. loss). [14]

Before the proof-of-stake model, the Ethereum protocol operated on a proof-of-work model, as originally pioneered in Bitcoin [15]. One of the key reasons for transitioning to a proof-of-work system was to reduce the energy consumption of the network, resulting in a reduction of 99.95%, essentially fixing one of the most widely criticized elements in blockchain consensus systems. [14]. The proof-of-stake system also has a lower rate of issuance of new ether, which is important in the context of aggregate supply changes.

The supply change rate, or alternatively, the net issuance rate, is the most significant single variable in this thesis and will be applied later in option valuations. Net issuance can be divided into two different mechanisms: 1) issuance and 2) burn. The issuance is simply the creation of new ETH that did not previously exist. In the early proof-of-work era 2015 - 2018, the issuance varied between 17 000 and 29 000 ETH per day, decreasing by time. In the recent proof-of-work era 2019 - 2022, the issuance was approximately 13 000 ETH per day. Since the Merge, the issuance has

been approximately 1 700 ETH per day, a 88% reduction in the issuance rate. The respective issuance percentage rates ranged from 7% to 15% in 2015 - 2018, 4% - 5% in 2015 - 2022, and around 0.5% after Merge. The initial total ETH supply was approximately 72 000 000 at launch in July 30, 2015 in the "Frontier" release, growing to 120 520 000 at the time of the Merge in September 15, 2022. [16]

Ethereum also has a burn mechanism that results in ongoing deflationary pressures in total supply. This mechanism has been in the protocol since August 2021 after the implementation of the "London" upgrade. The upgrade included a widely debated element called EIP-1559, the burn mechanism. EIP stands for Ethereum Improvement Proposal. The burn mechanism takes a part of the transaction fee and automatically removes it from circulation. Essentially, the motivation was to improve Ethereum's financial sustainability by introducing a platform take rate, resulting in a counterforce to the inflation caused by the issuance rate. The amount of gas burned is also a function of the network activity; the higher the demand for gas, the higher the burn. [16] To summarise,

$$\textit{Supply change rate} = \textit{Net issuance rate} = \textit{Issuance rate} - \textit{Burn rate}. \tag{1}$$

The total historical supply of Ethereum and the change rate of supply are also shown in Figure 1 [17]. Etherscan is used as the data source, as it is considered the most reputable Ethereum blockchain data explorer.

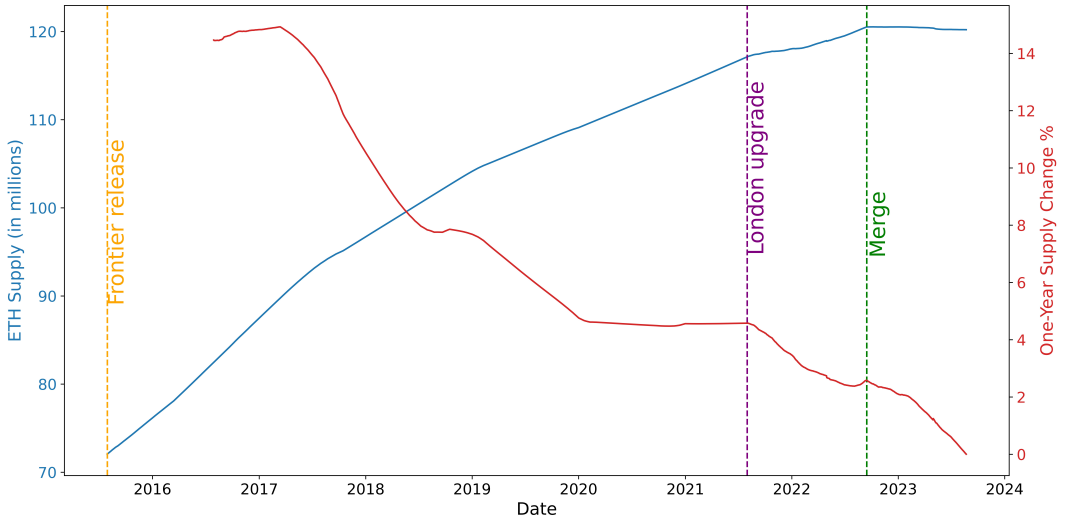

Figure 1: Ethereum supply and one-year supply change

Figure 1 shows how the total Ethereum supply has increased until the Merge in September 15, 2022, from which point on it has slightly decreased. The one-year supply change shows how inflation has steadily decreased as time passes.

2.3 ETH as a financial asset

ETH is a financial asset that has a market value and is actively traded on global markets. ETH and other crypto tokens are often referred to as crypto assets. In finance, crypto assets are a nascent asset class with a total market capitalisation of $1.1 trillion [11]. ETH's market capitalisation is $200 billion. The daily spot trading volumes of ETH range significantly depending on market conditions, but historically are in the tens of billions of dollars [11]. Figure 2 shows the historical development of ETH market capitalisation.

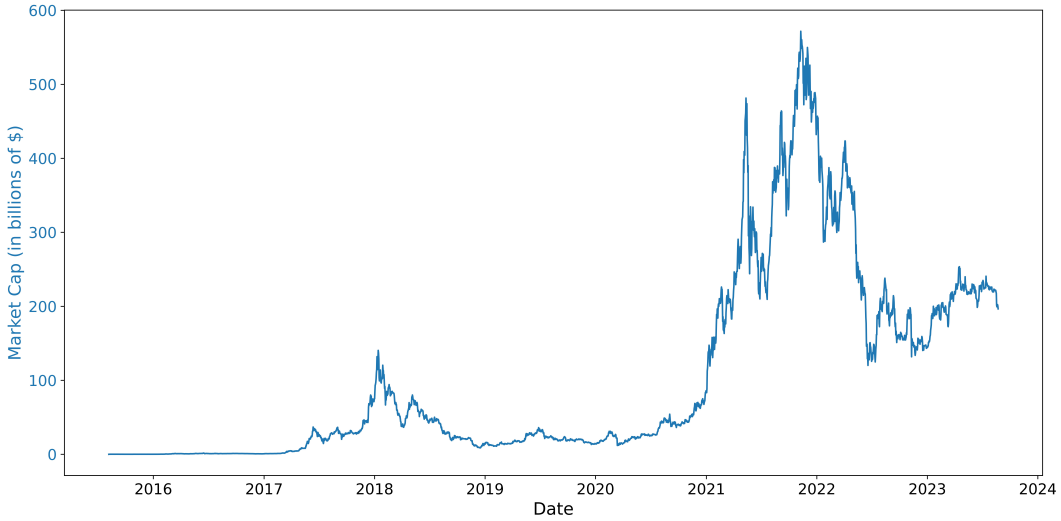

Figure 2: Ether market capitalisation over time

ETH has unique characteristics as an asset class but has elements of a currency, a commodity, and a security. The crypto asset can be considered a currency from the perspective that it can be simply transacted with in the Ethereum economy. If a party is willing to sell goods or services in exchange for ETH payments, the technology enables this activity. Arguably, the current major limiting factor for this use case is historical volatility. ETH can also be considered a commodity comparable to oil in the physical world since ETH is "computational fuel", as explained in Section 2.2. Lastly, ETH can be considered a security specifically after the London upgrade, since the burn mechanism is basically a value capture mechanism for the protocol. The burn rate can be compared to a traditional take rate of any marketplace business, and related financial metrics can be constructed. These financial metrics include widely used security valuation multiples, such as P/E ratios [18]. Moreover, there have been arguments that ETH could be considered a perpetual bond or an "Internet bond" due to the never-maturing periodic staking yield in the Ethereum protocol [19]. This yield is comparable to bond coupon payments, where the payment intervals are Ethereum block times. This distinction can be important from a valuation perspective; however, legally bonds are debt obligations and, thus, financial securities. Further, an important

distinction here is that the yield actually goes to ETH stakers that own "staked ETH", not to passive ETH holders. This thesis strictly studies the ETH asset.

Wide disagreement and different interpretations of the legal status of ETH exist among financial authorities, such as the U.S. Securities and Exchange Commission (SEC) and the U.S. Commodity Futures Trading Commission (CFTC). In a 2018 speech by the SEC's Director, William Hinman, the view was given that "current offers and sales of ETH are not securities transactions", widely interpreted as the SEC viewing ETH not as a security [20]. On the other hand, CFTC chairman Heath Tarbert directly stated in 2019 that the agency views ETH as a commodity and may allow ETH futures to trade on US markets (they are allowed today) [21]. The current SEC Director, Gary Gensler, has taken a different stance than the predecessor, not directly stating, but on various occasions suggesting that crypto assets may be securities [22]. Furthermore, on 6 June 2023, the SEC sued one of the largest and publicly listed crypto exchanges in the world, Coinbase, for operating as an unregistered securities exchange, broker, and clearing agency [23]. In particular, the SEC had approved Coinbase's public direct listing on the Nasdaq in April 2021, two years earlier, highlighting the lack of legal clarity of various crypto assets in the US [24]. Globally, increasingly many financial authorities have published legal crypto asset frameworks, such as the EU in June 2023 through its Market in Crypto Assets Regulation Act (MiCA), paving the way for clarity for crypto assets like Ethereum [25].

2.4 Derivative and option markets for ETH

Derivatives markets exist naturally as a result of a considerable volume of spot trading. In March 2023, crypto derivatives represented approximately 75% of the total crypto trading volume of $2.95 trillion [26]. According to Block, a reputable crypto data analytics provider, the total monthly trading volume of ETH options has ranged between $6.5 billion to $15 billion in 2023 [27]. The estimates consider the leading centralised ETH options exchanges, Deribit, CME Group, OKX, Delta Exchange, and Binance. In particular, decentralized option protocols, such as Hegic Options or Opyn are excluded from these estimates, because of their low comparable volumes. These protocols are examples of decentralised applications that are built on the Ethereum protocol, a concept introduced earlier.

Deribit is by far the largest ETH options exchange by volume, having a market share of approximately 80% between January and July in 2023 [27]. Despite CME Group being a global institution in traditional finance, it has not yet reached significant volumes of trading for ETH options. CME Group launched its ETH option product in August 2022 and the cumulative trading volume to date (August 2023) is estimated at $2 billion [27]. Consequently, the empirical analysis of this thesis will be based on Deribit's ETH options data.

2.5 Ethereum options literature

There exists research on both Ethereum as a system and options as financial derivatives. However, the literature at the intersection of these two areas remains underdeveloped. Ethereum was launched in 2013, while options theory can be considered to have its beginnings in the early 20th century with Bachelier's "Théorie de la spéculation" in 1900 [5]. Thus, the existing literature is heavily weighted in availability towards options.

However, some specific research has been done on the Ethereum options. Recently, Sapna and Mohan have published papers on the performance of numerical approximations in estimating the implied volatility structures of Ethereum options using the BSM model [28] [29]. The main idea in the construction of implied volatilities is to numerically solve the equation $C_{BSM} = C_{market}$, using techniques such as the Newton-Raphson method or the bisection method. Numerical root-finding methods are used because the equation does not have analytical solutions for volatility. Their research does not separately consider the supply changes in Ethereum and its effects on implied volatilities. They have used the Deribit options data, which provides further legitimacy to the data source also used in this thesis.

Considering other crypto assets, research is primarily focused on Bitcoin due to its largest market capitalisation and significance in the crypto industry. Hou et al. researched Bitcoin options in their 2020 study "Pricing Cryptocurrency Options" [30]. The study focused mainly on the correlation of price jumps and volatility and did not use the BSM model. In 2019, Pagnottoni published a paper on how neural networks could be applied to the pricing of Bitcoin options, but this study also does not consider the BSM model [31].

3 Options

This section reviews the literature on options and the mathematical principles for constructing the Black-Scholes-Merton model. The complete step-by-step proof of the BSM model is long; therefore, some of the intermediate steps are left out of Section 3.2, especially related to simple algebraic operations.

3.1 Stochastic calculus

Financial mathematics is based on stochastic calculus. Stochastic calculus is a branch of mathematics for quantifying uncertainty through the use of probabilities. The following sections are built to form a logical flow for the construction of the BSM model.

3.1.1 Probability theory

Probability theory is largely based on measures. This section introduces general notions of probability theory with the assumed basic knowledge of the concepts of measures. The main references in this section include Durrett and Kytola [32] [33]. There are many reputable books in probability theory, including Jacod (2004) and Williams (1991), which introduce the same concepts with alternative notation. [34] [35]

An *outcome* ω of a random experiment represents a single realization of randomness. The sample space Ω is the set that consists of all possible outcomes.

An *event* E is a subset $E \subset \Omega$ of the set of possible outcomes. The event E is said to occur if $\omega \in \Omega$ belongs to this subset, i.e., if $\omega \in E$. All subsets of Ω cannot be allowed as events, but a suitable collection $\mathcal{F}$ of subsets needs to be constructed, consistent with the axioms of probability.

A *probability space* is a triple $(\Omega, \mathcal{F}, P)$, where Ω is a set of outcomes, $\mathcal{F}$ is a collection of events, and $P : \mathcal{F} \to [0, 1]$ is a function that assigns probabilities to events. The collection $\mathcal{F}$ is a σ-field (or σ-algebra). A collection $\mathcal{F} \subset \mathcal{P}(\Omega)$ of subsets of a set Ω is a σ-algebra on Ω if

1. $\Omega \in \mathcal{F}$,
2. if $E \in \mathcal{F}$ then $E^{\mathbf{c}} = \Omega \backslash E \in \mathcal{F}$,
3. if $E_1, E_2, \ldots \in \mathcal{F}$ then $\bigcup_{n \in \mathbb{N}} E_n \in \mathcal{F}$. [32]

Probability spaces form the basis of stochastic calculus. In addition to this concept, random variables and expected values are found in standard textbooks.

Let $\mathbf{R}^d$ be the set of vectors $(x_1, \ldots x_d)$ of real numbers and $\mathcal{R}^d$ be the Borel sets, the

smallest σ-field containing the open sets. Let $(S, \mathcal{S})$ be an arbitrary measurable space. A function $X : \Omega \to S$ is said to be a measurable map from $(\Omega, \mathcal{F})$ to $(S, \mathcal{S})$ if

$$X^{-1}(B) \equiv \{\omega : X(\omega) \in B\} \in \mathcal{F} \text{ for all } B \in \mathcal{S}.$$

If $(S, \mathcal{S}) = \left(\mathbf{R}^d, \mathcal{R}^d\right)$ and $d > 1$, then X is called a random vector. If $d = 1$, X is called a *random variable*. [33]

The *expected value* $\mathbb{E}[X]$ of a random variable $X : \Omega \to S \subset \mathbb{R}$, represents an average of the possible values of X over all randomness, weighted according tow probabilities P. If X is a real-valued random variable defined on a probability space $(\Omega, \mathcal{F}, \mathrm{P})$, the expected value of X is defined as the Lebesgue integral

$$\mathbb{E}[X] = \int_{\Omega} X d\mathrm{P}.$$

3.1.2 Stochastic processes

The references in this section include Karatzas and Shreve (1991), Peltola (2023), and Kaila (2008) [36][37][38]. There is a broad literature on stochastic processes; well-known resources include Ross (1995) and Parzen (1999). [39] [40]

A stochastic process is a collection of real valued random variables $(X_t)_{t\geq 0}$ defined on a probability space $(\Omega, \mathcal{F}, P)$. Equivalently, a stochastic process is a collection of random variables $X = \{X_t; 0 \leq t < \infty\}$ on a sample space $(\Omega, \mathcal{F})$, which take values in a second measurable space $(S, \mathcal{S})$, called the state space. [36]

Three fundamental concepts in stochastic processes are filtration, the Markov property, and the martingale property. *Filtration* attempts to mathematically formalize the notion of "information". It basically refers to the information available at time t. A collection $\mathcal{F}_\bullet = (\mathcal{F}_n)_{n\in\mathbb{N}_0}$ comprising an increasing family $\mathcal{F}_0 \subset \mathcal{F}_1 \subset \cdots \subset \mathcal{F}$ of sub-sigma-algebras of $\mathcal{F}$ is called a filtration. The related tuple $(\Omega, \mathcal{F}, \mathcal{F}_\bullet, P)$ is called a *filtered probability space*. [37] A stochastic process $(X_t)_{t\geq 0}$ *is adapted to* the filtration $(\mathcal{F}_t)_{t\geq 0}$, if the stochastic process X_t is $\mathcal{F}_t$-measurable for every t. [41]

A stochastic process $\{X_t\}_{t\geq 0}$ on a filtered probability space $(\Omega, \mathcal{F}, \mathcal{F}_\bullet, P)$ is called a *martingale* with respect to a filtration $\mathcal{F}_\bullet$ (and with respect to P) if

1. X_t is $\mathcal{F}_t$-measurable for all t,
2. $\mathbb{E}\left[|X_t|\right] < \infty$ for all t,
3. $\mathbb{E}\left[X_t \mid \mathcal{F}_s\right] = X_s$ for all $t \geq s$. [41]

Essentially, a martingale is a stochastic process, where the conditional expectation of the next value of the sequence is equal to the present value. For example, if we assume

that a stock price is a martingale, the best forecast of the future value of the stock, at any given future time t, is its current value X_s.

A *Markov process* is a stochastic process for which only the present value of the random variable matters when trying to forecast the future. An $(\mathscr{F}_t)_{t\geq 0}$-adapted process $(X_t)_{t\geq 0}$ is a Markov process if

$$\mathbb{E}[X_t \mid \mathscr{F}_s] = \mathbb{E}[X_t \mid X_s] \quad \text{for all } 0 \leq s \leq t. \tag{2}$$

Equation (2) is often referred to as the *Markov property*. [38]

Although martingales and Markov processes are intimately related, they have different mathematical definitions. Martingales can sometimes be constructed from Markov processes under certain conditions, and certain Markov processes possess the martingale property under specific filtrations. In financial mathematics, the stock price process under the risk-neutral measure is a martingale, and when modeling stock prices (as in the BSM model), the Markov property becomes crucial.

3.1.3 Brownian motion

The references for this section include Karatzas and Shreve (1991), Peltola (2023) and Le Gall (2016) [42].

Brownian motion is both a martingale and a Markov process. It is one of the fundamentally important stochastic processes, originally developed in the 19th century in the context of diffusion phenomena in physics and as a way to model the behavior of financial markets [37].

Mathematically, Brownian motion is a continuous-time real-valued stochastic process usually denoted $B = (B_t)_{t\geq 0}$, defined on some probability space $(\Omega, \mathscr{F}, P)$. More precisely, a Brownian motion with a starting point x_0 has the following properties:

1. For each $\omega \in \Omega$, $B_0(\omega) = x_0$.
2. For any partition $0 \leq t_0 < t_1 < \ldots < t_n$, the increments

   $$\left\{B_{t_{j+1}} - B_{t_j} \mid j = 0, 1, \ldots, n-1\right\}$$

   are independent random variables.
3. For each $0 \leq s < t$, the increment $B_t - B_s$ has Gaussian distribution that only depends on the time difference

   $$B_t - B_s \sim \mathcal{N}(0, t-s), \quad 0 \leq s < t.$$

4. $\mathbb{P}$-almost every sample path $t \mapsto B_t$ is continuous

$$\mathbb{P}\left[\{\omega \in \Omega \mid t \mapsto B_t(\omega) \text{ is continuous }\}\right] = 1.$$

[37]

In the context of financial markets and this thesis, the assumption that the stock price process follows a geometric Brownian motion (GBM) is the fundamental building premise to use the BSM model.

A stock price process S_t following the GBM satisfies the following stochastic differential equation:

$$dS_t = \mu S_t dt + \sigma S_t dB_t, \tag{3}$$

where B_t is Brownian, μ is drift, and σ is volatility.

3.1.4 Itô's calculus

Before moving to option pricing theory, we last introduce critical concepts in stochastic calculus from the mathematician Itô, which originated in the 1940s. Itô essentially developed a generalization of integration by parts to stochastic integrals. The process and lemma are presented.

ltô process I_t is a stochastic process with a drift term and a stochastic term:

$$dI_t = a\left(I_t, t\right) dt + b\left(I_t, t\right) dB_t, \tag{4}$$

where the drift $a\left(I_t, t\right)$ and the volatility $b\left(I_t, t\right)$ are functions of I_t and t, and B_t is Brownian motion. [41]

ltô's Lemma states the following: Let $X^{(1)}, X^{(2)}, \ldots, X^{(d)}$ be continuous semimartingales and $f : \mathbb{R}^d \to \mathbb{R}$ twice continuously differentiable. Define $\vec{X}_t = \left(X_t^{(1)}, \ldots, X_t^{(d)}\right)$. Then, the following formula holds

$$f\left(\vec{X}_t\right) - f\left(\vec{X}_0\right) = \sum_{j=1}^{d} \int_0^t \left(\partial_j f\right)\left(\vec{X}_s\right) \mathrm{d}X_s^{(j)} + \frac{1}{2} \sum_{j,k=1}^{d} \int_0^t \left(\partial_j \partial_k f\right)\left(\vec{X}_s\right) \mathrm{d}\left\langle X^{(j)}, X^{(k)} \right\rangle_s, \quad t \geq 0 \tag{5}$$

where $\left\langle X^{(j)}, X^{(k)} \right\rangle$ denotes the quadratic covariation between $X^{(j)}$ and $X^{(k)}$. [37] [43]

Critically, every martingale is a semimartingale (but not vice versa), and Brownian motion is a martingale as previously discussed. Thus, Itô's Lemma can be used as a tool in the options calculations.

3.2 Option pricing

This section presents the literature related to the BSM model and constructs the model using the tools of Section 3. Longer algebra sections are omitted to maintain a reasonable scope in the thesis. The math sections are presented in logical continuation.

Quantitative finance has a wide literature. References include Paul Wilmott's quantitative finance books (2001, 2006), and Baxter and Rennie (2006), which all include mathematics around the BSM model [44][45][46].

3.2.1 Black-Scholes in differential form

First, the key assumptions about the markets are presented below:

1. There is no arbitrage opportunity (i.e. the markets are perfectly efficient).
2. Any market participant can borrow and lend any amount at the riskless rate (infinite liquidity).
3. Any market participant can buy and sell any amount of the stock (infinite stock supply).
4. No transaction costs (i.e. perfectly frictionless market).

Next, assume the stock price S_t follows a geometric Brownian motion:

$$dS_t = \mu S_t dt + \sigma S_t dB_t, \tag{6}$$

where S_t is the stock price at time t, μ is the expected return, σ is the volatility, and B_t is Brownian.

Equation (6) can be shown to satisfy

$$S_t = S_0 e^{(\mu - \frac{\sigma^2}{2})t + \sigma B_t} \sim \mathcal{LN}\left(S_0 e^{\mu t}, S_0^2 e^{2\mu t}(e^{\sigma^2 t} - 1)\right), \tag{7}$$

where $\mathcal{LN}$ is the lognormal distribution.

Now, we assume a risk-neutral world, where $\mu = r$, the risk-free rate. Then the process becomes:

$$dS_t = rS_t dt + \sigma S_t dB_t, \tag{8}$$

where r is the risk-free rate and other variables defined as in Equation (6).

Consider a European call option on this stock with strike price K and maturity T. Let $C(t, S_t)$ be the price of this option at time t when the stock price is S_t.

By Itô's Lemma from Equation (5), $C(t, S_t)$ satisfies the following stochastic differential equation

$$dC(t, S_t) = \frac{\partial C}{\partial t} dt + \frac{\partial C}{\partial S} dS_t + \frac{1}{2} \frac{\partial^2 C}{\partial S^2} (dS_t)^2. \tag{9}$$

Inserting the geometric Brownian motion in Equation (8) for dS_t into Equation (9) yields

$$dC(t, S_t) = \frac{\partial C}{\partial t}dt + \frac{\partial C}{\partial S}(rS_t dt + \sigma S_t dB_t) + \frac{1}{2}\frac{\partial^2 C}{\partial S^2}(\sigma^2 S_t^2 dt). \tag{10}$$

Simplifying, we get

$$dC(t, S_t) = \left(\frac{\partial C}{\partial t} + rS_t\frac{\partial C}{\partial S} + \frac{1}{2}\sigma^2 S_t^2\frac{\partial^2 C}{\partial S^2}\right)dt + \sigma S_t\frac{\partial C}{\partial S}dB_t. \tag{11}$$

The last stochastic term in Equation (11) including Brownian motion B_t can be eliminated by selecting a portfolio of $\Pi = -C + \frac{\partial C}{\partial S}S_t$, and noticing that resulting portfolio change must be riskless during a time differential, yielding the risk-free rate

$$d\Pi = \left(-\frac{\partial C}{\partial t} - \frac{1}{2}\frac{\partial^2 C}{\partial S^2}\sigma^2 S_t^2\right)dt = r\Pi dt. \tag{12}$$

Inserting the selected portfolio into Equation (12) gives

$$\frac{\partial C}{\partial t} + \frac{1}{2}\sigma^2 S_t^2\frac{\partial^2 C}{\partial S^2} + rS_t\frac{\partial C}{\partial S} - rC(t, S_t) = 0, \tag{13}$$

which is the differential form of the basic Black-Scholes model for European call options. Note that the stock does not pay dividends in the basic BS model; it will be discussed in Section 3.2.3 in detail.

3.2.2 Black-Scholes closed solutions

Equation (13) is a second-order partial differential equation with the following boundary conditions:

1. **At expiry** ($t = T$): The payoff of the option is given by the difference between the stock price and the strike price at expiry. The first boundary condition is:

$$C(T, S) = \max(S - K, 0). \tag{14}$$

2. **Stock price approaches zero** ($S \to 0$): The call option becomes worthless if the stock price goes to zero. The second boundary condition is:

$$C(t, 0) = 0. \tag{15}$$

3. **Stock price approaches infinity** ($S \to \infty$): The option price increases together with an increasing stock value, subtracted by the present value of the strike price, leading to the third boundary condition:

$$C(t, S) \to S - Ke^{-r(T-t)} \quad \text{as} \quad S \to \infty. \tag{16}$$

The problem can be tackled with various approaches, such as direct integration, by applying the Feynman-Kac theorem, using the Capital Asset Pricing Model (CAPM), or by transforming Equation (13) into the heat equation, as originally done by Black and Scholes [2] [47].

The intermediate steps to the final form are omitted to maintain the scope of the thesis. The closed solution of Equation (13) is the basic Black-Scholes formula for a European call option (C) on a non-dividend paying stock and is given as

$$C = S_0\mathcal{N}(d_1) - Ke^{-rt}\mathcal{N}(d_2), \tag{17}$$

where

- C is the price of the call option
- S_0 is the initial stock price
- K is the strike price
- t is the time to maturity
- r is the risk-free interest rate.

In Equation (17), $\mathcal{N}$ is the cumulative distribution function of the standard Gaussian, defined as

$$\mathcal{N}(z) = \frac{1}{\sqrt{2\pi}} \int_{-\infty}^{z} e^{-\frac{x^2}{2}} dx. \tag{18}$$

The parameters d_1 and d_2 are calculated as

$$d_1 = \frac{ln(\frac{S_0}{K}) + (r + \frac{\sigma^2}{2})t}{\sigma\sqrt{t}}, \tag{19}$$

$$d_2 = d_1 - \sigma\sqrt{t}, \tag{20}$$

where σ is the volatility of the stock's returns.

3.2.3 Merton dividends adjustment and BSM

In the 1973 published paper "Theory of Rational Option Pricing", Merton provided a framework on how the basic Black-Scholes model (Equations (17)-(20)) can be extended to account for dividends [48]. These concepts are also discussed later in his 1991 foundational text book, "Continuous-Time Finance" [49].

The main idea is to assume that dividends are continuous and to use a slightly adjusted geometric Brownian stock price process

$$dS_t = rS_t dt - qS_t dt + \sigma S_t dB_t = (r - q)S_t dt + \sigma S_t dB_t, \tag{21}$$

where q is the continuous dividend yield of the underlying stock, and other variables defined as in Equation (8). If the stock pays dividends continuously at a rate q, then over a time differential dt, the amount of dividends paid is $qS_t dt$, where S_t is the stock price at time t. Because dividends are cash paid out of a company, this has a negative effect on the stock price S_t.

The stock price process is also lognormally distributed as in Equation (7), with slight adjustments to the expected value and variance:

$$S_t \sim \mathcal{LN}\left(S_0 e^{(r-q)t}, S_0^2 e^{2(r-q)t}(e^{\sigma^2 t} - 1)\right), \tag{22}$$

where variables are defined as in Equations (7) and (21).

Applying the algebra of Sections 3.2.1 - 3.2.2 gives the dividend-adjusted BSM model. Specifically, the Black-Scholes-Merton formula for a European call option (C) on a dividend paying stock is given as

$$C = S_0 e^{-qt}\mathcal{N}(d_1) - Ke^{-rt}\mathcal{N}(d_2), \tag{23}$$

where

- C is the price of the call option
- S_0 is the initial stock price
- K is the strike price
- t is the time to maturity
- r is the risk-free interest rate
- q is the continuous dividend yield.

In Equation (23), $\mathcal{N}$ is the cumulative distribution function of the standard Gaussian, defined as

$$\mathcal{N}(z) = \frac{1}{\sqrt{2\pi}} \int_{-\infty}^{z} e^{-\frac{x^2}{2}} dx. \tag{24}$$

The parameters d_1 and d_2 are calculated as

$$d_1 = \frac{ln(\frac{S_0}{K}) + (r - q + \frac{\sigma^2}{2})t}{\sigma\sqrt{t}}, \tag{25}$$

$$d_2 = d_1 - \sigma\sqrt{t}, \tag{26}$$

where σ is the volatility of the stock's returns.

As can be seen, the model is close to the version without dividends in Equations (17)-(20), except for the presence of the q-term. Considering the research questions of

the thesis, it is important to further elaborate the notion of dividends. The dividend yield of a company is defined as

$$q = \frac{\text{Annual dividends per share}}{\text{Price per share}}. \tag{27}$$

Equivalently,

$$q = \frac{\text{Annual total dividends}}{\text{Company market capitalisation}}. \tag{28}$$

Due to the assumption of continuity of q in the BSM model, it is used more accurately for option indices where dividends are paid out in a rate of approximately continuously.

4 Research methods

The aim of this section is to connect the unique characteristics of Ethereum with the BSM model. In Section 4.1 a novel approach is presented to value ETH options that incorporates supply dynamics into the equations. Moreover, Sections 4.2 - 4.3 outline how the comparison analysis of the thesis is conducted.

4.1 Modified BSM for Ethereum options

The main argument in this section is that crypto asset supply changes are simply another form of value-affecting mechanism for those who have an exposure to the underlying. Formulas are provided to justify the claims.

Recall that the initial problem was that there was no parameter to account for supply changes in the BSM model for Ethereum. Supply changes are unique characteristics of crypto assets that clearly have an effect on the underlying asset, and therefore also on any derivative of the underlying. The supply change equation was introduced as an idea in Equation (1). A mathematical justification for the claims is presented in Section 4.1.1, and the modified BSM model for crypto assets is formalized in Section 4.1.2.

4.1.1 Mathematical formulation

Consider again the following stock price process, including dividends, presented in Section 3.2.3, i.e.,

$$dS_t = rS_t dt - qS_t dt + \sigma S_t dB_t.$$

Over a time differential dt, the amount of dividends paid is $qS_t dt$. At time $t + dt$, the stock is worth $S_t + dS_t$, and existing shareholders experience a relative change in stock value of

$$\begin{aligned} &\frac{S_{t+dt} - S_t}{S_t} \\ &= \frac{S_t + dS_t - S_t}{S_t} \\ &= \frac{rS_t dt - qS_t dt + \sigma S_t dB_t}{S_t} \\ &= r dt + \sigma dB_t - q dt, \end{aligned} \tag{29}$$

where $-qdt$ represents the stock value dilution caused by dividends. As a concrete example, over a year period, share value would be diluted by a factor of $-q$. That is, existing shares are diluted by $(q * 100)\%$ over a period of one year due to dividends.

Now, assume that a company has a constant market capitalisation M and increases the amount shares at a continuous rate. Let N_t be amount of shares at time t, and s the rate of change of the amount of shares. Consequently, the stock price S_t can be

expressed as $S_t = {}^{M}/_{N_t}$.

The differential equation describing the change in the amount of shares is

$$dN = sN_t dt, \tag{30}$$

where the variables are defined as above.

Over a time differential dt, the amount of new shares created is $sN_t dt$. At time $t + dt$, the total amount of shares in existence is $N_t + dN_t$. Existing shareholders experience a share value dilution of

$$\begin{aligned}
&\frac{S_{t+dt} - S_t}{S_t} \\
&= \frac{\frac{M}{N_{t+dt}} - \frac{M}{N_t}}{\frac{M}{N_t}} \\
&= \frac{N_t - N_{t+dt}}{N_{t+dt}} \\
&= \frac{N_t - (N_t + dN_t)}{N_t + dN_t} \\
&= \frac{-dN_t}{N_t + dN_t} \\
&= \frac{-sN_t dt}{N_t + sN_t dt} \\
&= -\frac{sdt}{1 + sdt},
\end{aligned} \tag{31}$$

which mathematically differs from the dilution created by dividends in Equation (29). As a concrete example, over a two-year period, the share value would be diluted by a factor of ${}^{-2s}/_{(1+2s)}$. That is, existing shares are $({}^{2s}/_{(1+2s)}) * 100\%$ less valuable over a period of two years.

As a result, the comparable GBM stock price process including a continuous increase in the amount of shares and without dividends is given by

$$dS_t = rS_t dt - \frac{s}{1 + sdt} S_t dt + \sigma S_t dB_t, \tag{32}$$

where the term ${}^{s}/_{(1+sdt)}$ is the stock dilution scaling factor dependent on the time differential dt, which means the scaling factor is not a scalar.

Equation (32) can be written as

$$dS_t = rS_t dt - \frac{1}{1 + sdt} sS_t dt + \sigma S_t dB_t, \tag{33}$$

which is closer to the original form of Equation (21), except for the non-scalar drift scaling factor ${}^{1}/_{(1+sdt)}$.

We conclude that both dividends and increases in the share amount have a diluting effect on the underlying stock price under the given assumptions, but the dilution factors and stock price processes are different.

Lastly, the use of Equation (33) would not necessarily result in any known version of the BSM model due to the non-scalar drift scaling factor. However,

$$\lim_{s \to 0} \frac{1}{1 + sdt} = 1, \tag{34}$$

and for small values of s it holds that

$$\frac{1}{1 + sdt} \approx 1 - sdt. \tag{35}$$

Equation (34) holds trivially and for Equation (35), consider an n:th order Taylor approximation at point $a = 0$:

$$f(x) \approx f(0) + f'(0)x + \frac{f''(0)}{2!}x^2 + \ldots + \frac{f^{(n)}(0)}{n!}x^n, \tag{36}$$

where $f(x) = \frac{1}{1+x}$ and $x = sdt$. Equation (36) simplifies to a known geometric series:

$$\begin{aligned} f(x) &\approx 1 - x + x^2 - x^3 + \ldots + (-1)^n x^n \\ &= 1 - sdt + (sdt)^2 - (sdt)^3 + \ldots + (-1)^n (sdt)^n \\ &= 1 - sdt, \end{aligned} \tag{37}$$

because the differential terms $(dt)^n$ become negligibly small for $n \geq 2$. These details are important when constructing the crypto asset BSM in Section 4.1.2.

4.1.2 Crypto asset BSM

In this section we connect Equation (1) to Equation (33) and construct a suitable BSM version for Ethereum.

Assume that we have a non-dividend-paying crypto asset with price Q_t and with an annual issuance rate $i \geq 0$ and an annual burn rate of b, where $0 \leq b < 1$. Denote the net issuance by I_N, $I_N \in \mathbb{R}$. Then, by Equation (1):

$$I_N = i - b, \tag{38}$$

where variables are defined above.

Mathematically, crypto asset supply changes are comparable to stock supply changes discussed in Section 4.1.1. This is given as a premise since it is trivially true. Moreover, crypto asset price processes can be modeled using GBM due to the widespread use of the traditional BSM model in crypto option markets. Using Equation (33), we can state the crypto asset price process explicitly as

$$\begin{aligned} dQ_t &= rQ_t dt - \frac{1}{1 + I_N dt} I_N Q_t dt + \sigma Q_t dB_t \qquad (39) \\ &= rQ_t dt - \frac{1}{1 + (i-b)dt}(i-b)Q_t dt + \sigma Q_t dB_t \\ &= rQ_t dt - \frac{1}{1 + (i-b)dt} iQ_t dt + \frac{1}{1 + (i-b)dt} bQ_t dt + \sigma Q_t dB_t, \qquad (40) \end{aligned}$$

where $1/(1+(i-b)dt)$ is the non-scalar drift scaling factor of the price effect caused by issuance i and burn b and other variables defined as before. Importantly, we cannot state that this process is necessarily a geometric Brownian without further examination.

To apply this crypto asset price process to the BSM model, we apply the Taylor approximation from Equation (35) to Equation (39)

$$\begin{aligned} dQ_t &\approx rQ_t dt - (1 - I_N dt) I_N Q_t dt + \sigma Q_t dB_t \\ &= rQ_t dt - I_N Q_t dt + I_N^2 Q_t (dt)^2 + \sigma Q_t dB_t \\ &= rQ_t dt - I_N Q_t dt + \sigma Q_t dB_t \\ &= (r - i + b)Q_t dt + \sigma Q_t dB_t, \qquad (41) \end{aligned}$$

where variables are defined as before.

Equation (41) is now comparable to the original geometric Brownian of Merton in Equation (21), with different scalar multipliers. Consequently, the post-approximation Q_t is lognormal with a net issuance-adjusted expected value and variance:

$$Q_t = Q_0 e^{(r-i+b-\frac{\sigma^2}{2})t + \sigma B_t} \sim \mathcal{LN}\left(Q_0 e^{(r-i+b)t}, Q_0^2 e^{2(r-i+b)t}(e^{\sigma^2 t} - 1)\right), \tag{42}$$

where variables are defined as previously.

The BSM model can now be generalized to crypto assets:

The Black-Scholes-Merton formula for a European call option (C) on a non-dividend paying crypto asset with continuous token issuance and continuous token burn is given as

$$C = Q_0 e^{-(i-b)t} \mathcal{N}(d_1) - K e^{-rt} \mathcal{N}(d_2), \tag{43}$$

where

- C is the price of the call option
- Q_0 is the initial crypto asset price
- K is the strike price
- t is the time to maturity
- r is the risk-free interest rate
- i is the continuous issuance rate
- b is the continuous burn rate

$\mathcal{N}$ is the cumulative distribution function of the standard Gaussian, defined as

$$\mathcal{N}(z) = \frac{1}{\sqrt{2\pi}} \int_{-\infty}^{z} e^{-\frac{x^2}{2}} dx. \tag{44}$$

The variables d_1 and d_2 are calculated as

$$d_1 = \frac{ln(\frac{Q_0}{K}) + (r - i + b + \frac{\sigma^2}{2})t}{\sigma\sqrt{t}}, \tag{45}$$

$$d_2 = d_1 - \sigma\sqrt{t}, \tag{46}$$

where σ is the volatility of the crypto asset's returns.

4.1.3 Model assumptions

The key assumption of the model is the use of the Taylor approximation, which means that its effects must be properly examined. The error is the difference between the function and the Taylor approximation. This can be explicitly written as

$$R_n(x) = \frac{f^{(n+1)}(c)}{(n+1)!}(x-a)^{n+1}, \tag{47}$$

where $f = {}^{1}/_{(1+x)}$ and c is some number between a and x.

The approximation of Equation (35) is equivalent to the first-order Taylor approximation at the point $a = 0$. Thus,

$$\begin{aligned} R_1(x) &= \frac{f''(c)}{2!}x^2 \\ &= (1+c)^{-3}x^2. \end{aligned} \tag{48}$$

We seek to construct the maximum error bounds to understand how the model behaves under different variations of net issuance and option expiration time.

For $x \geq 0$, since $0 \leq c \leq x$, $(1+c)^{-3} \leq 1$. Therefore, $|R_{1+}(x)| \leq x^2$. For $x < 0$, since $x \leq c \leq 0$, the upper error bound is at $c = x$. Therefore, $|R_{1-}(x)| \leq (1+x)^{-3}x^2$.

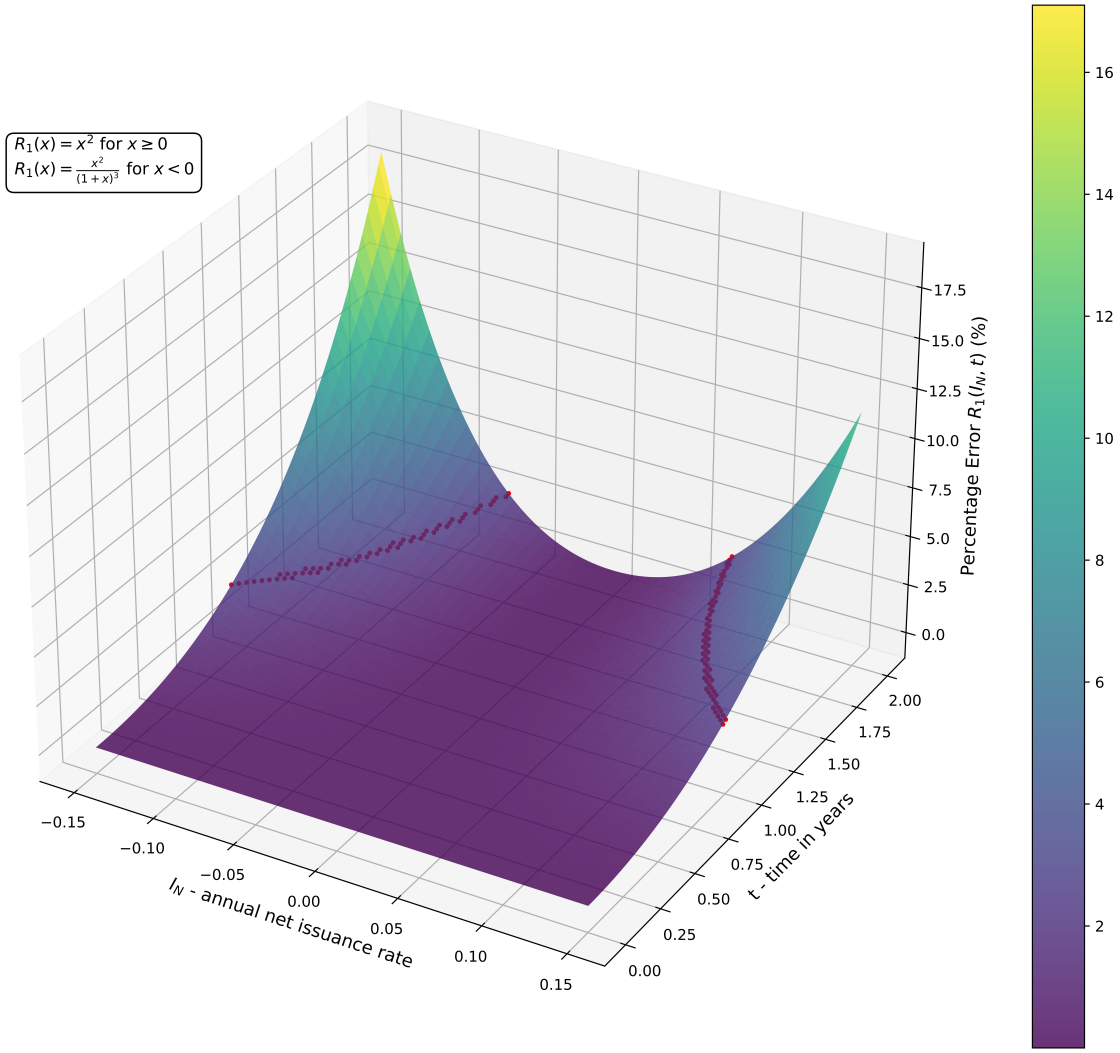

Figure 3: Taylor approximation percentage error bounds for $f = {}^{1}/_{(1+I_N t)}$. Red curved lines mark the intersection of a plane at $R_1 = 2.5\%$.

Figure 3 shows how the Taylor approximation error bounds behave for different parameter selections of net issuance I_N and option expiration time t. The red curved lines mark the intersection of a plane at $R_1 = 2.5\%$, under which 82% of the combinations of parameters are located. This can be interpreted as the approximation having a theoretical maximum error of 2.5% in 82% of the possible I_N and t combinations in the range $-0.15 \leq I_N \leq 0.15$ and $0 \leq t \leq 2$.

An examination of Figure 3 suggests that when the net issuance rate and the expiration time of the option increase, the approximation error increases. Furthermore, it is asymmetric in the sense that deeply negative issuance rates result in higher approximation errors than deeply positive rates. This is caused by the function $f = {}^{1}/_{(1+x)}$ not being symmetric around the y-axis itself. This can also be confirmed with math; Let T denote the Taylor approximation function, fix $t = 2$ and take $I_N = 0.10$ and $I_N = -0.10$

$$|f(0.2) - T(0.2)| = \left| \frac{1}{1+0.2} - (1 - 0.2) \right| = 0.033\ldots \tag{49}$$

$$\neq |f(-0.2) - T(-0.2)| = \left| \frac{1}{1-0.2} - (1 - (-0.2)) \right| = 0.05. \tag{50}$$

Using the idea of Figure 3, we construct Table 1 with varying ranges of I_N and option expiry time T.

$I_{N_{\text{min}}}$	$I_{N_{\text{max}}}$	T	R_1 error bound	Values under R_1
-0.15	0.15	2	1.0%	67.0%
-0.1	0.15	2	1.0%	73.1%
-0.05	0.1	2	1.0%	88.3%
-0.05	0.05	2	1.0%	99.6%
-0.15	0.15	2	2.5%	82.2%
-0.1	0.15	2	2.5%	87.8%
-0.05	0.1	2	2.5%	97.3%
-0.05	0.05	2	2.5%	100.0%
-0.15	0.15	5	2.5%	50.2%
-0.1	0.15	5	2.5%	55.7%
-0.05	0.1	5	2.5%	72.6%
-0.05	0.05	5	2.5%	88.5%
-0.15	0.15	5	5.0%	60.3%
-0.1	0.15	5	5.0%	66.5%
-0.05	0.1	5	5.0%	83.2%
-0.05	0.05	5	5.0%	96.8%

Table 1: R_1 error bounds for different ranges of I_N and t and the resulting percentage values under the R_1 plane.

Since January 2018, Ethereum has had a maximum positive net issuance rate of approximately 10% and a minimum negative net issuance rate of approximately -0.25% (Figure 1). Interpreting the Table 1, this corresponds to 97.3% of value combinations being acceptable with a 2.5% error bound, when the value ranges are $-0.05 \leq I_N \leq 0.10$ and $0 \leq t \leq 2$. If the option expiry time range is increased to $0 \leq t \leq 5$, the respective results are 72.6% acceptance with a 2.5% error bound, with the same I_N value ranges. Increasing the R_1 error bound to 5.0% results in 83.2% acceptance with the same value ranges.

To conclude, the Taylor approximation is suitable to be used in the model and works with neglible errors in most cases when using Ethereum's historical net issuance rates. The model is particularly accurate for short- and medium-term options, but can also be used for longer ones. However, if the option expiration time increases to more than 2 years, and especially if the net issuance rates are high simultaneously, numerical error analysis is worth conducting when using the model.

Finally, it is important to address the continuity assumption for the issuance rate i and the burn rate b. As discussed earlier, the dividend-adjusted BSM model is often applied for option indices, where the continuity approximation results in negligible errors. In the case of here, the model is directly suitable for individual crypto assets due to the concept of block times in blockchain protocols. As mentioned in Section 1.1, Ethereum's average block time is 12 seconds. Practically, this means that the Ethereum system updates its state every 12 seconds. Notably, there are blockchain protocols with considerably slower block times. The continuity approximation error ϵ can be written as

$$\begin{aligned} \epsilon &= \left| \left(1 + \frac{1}{B}\right)^B - \lim_{n\to\infty} \left(1 + \frac{1}{n}\right)^n \right| \\ &= \left| \left(1 + \frac{1}{B}\right)^B - e \right|, \end{aligned} \tag{51}$$

where B is the amount of blocks added to the blockchain in a year. B can be calculated from block times. In Ethereum, $B_{eth} \approx 2628000$, yielding

$$\begin{aligned} \epsilon_{eth} &= \left| \left(1 + \frac{1}{2628000}\right)^{2628000} - e \right| \\ &\approx 5 \times 10^{-7}. \end{aligned} \tag{52}$$

As a result, the contuinity assumption of issuance and burn rates hold comfortably for Ethereum and for any crypto asset with sufficiently small block times.

4.2 Data acquisition

This section explains the two main data sets used in the comparison analysis of the two different models, the original BSM and the crypto BSM. First, synthetic data are used to simulate how models should differ under theoretical circumstances. Secondly, ETH option market data is retrieved from Deribit options exchange to compare the models with real-world data.

4.2.1 Synthetic data

The synthetic data set is created with the following specifications:

The parameters for the crypto asset price (Q_t), risk-free rate (r), net issuance ($I_N = i - b$), and time to maturity (t) are set as 2000, 0, 0, and 1, respectively. A series of 31 strike prices (K_i) are linearly spaced between 500 and 3500. A volatility smile is simulated by generating a set of volatilities using a parabolic equation that is a function of the strike prices. The equation used is as follows,

$$\sigma_i(K_i) = 0.20 + 0.3\left(\frac{K_i - 2000}{1500}\right)^2, \quad i = 1, 2, \ldots, 31 \tag{53}$$

where $\sigma_i(K_i)$ denotes the volatility corresponding to the strike price K_i.

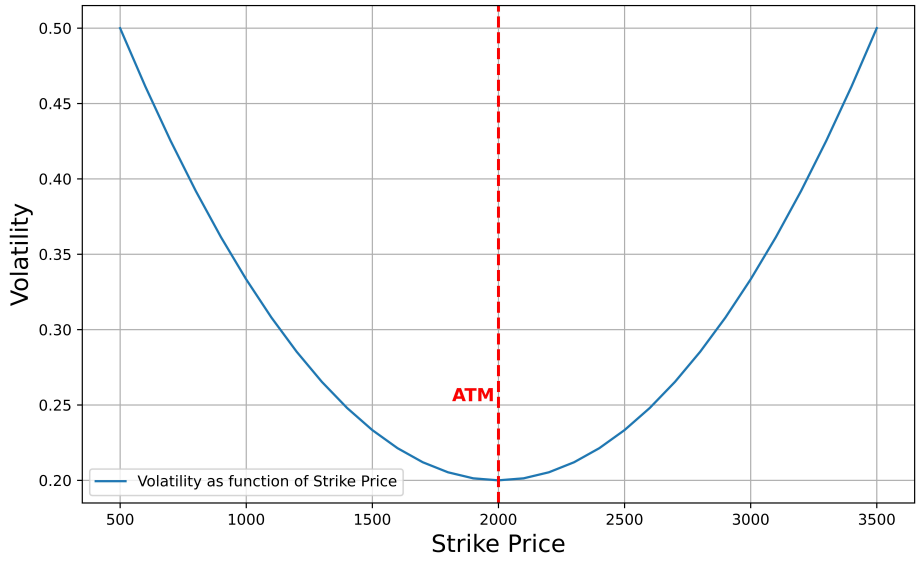

Figure 4: Synthetic volatility smile as a function of strike prices. ATM refers to "at-the-money", meaning the crypto asset spot price is $Q_t = 2000$.

Figure 4 visualizes the synthetic data set. The decision to simulate a "smile" for the volatilities is based on the fact that most implied volatilities in real-world market

data form a parabolic shape. In other words, there is a natural tendency for implied volatilities to increase for deep out-of-the-money (OTM) or in-the-money (ITM) options. This phenomenon is rooted in the differences in the market distribution of returns compared to the normal distribution, namely that the market distribution tails have more probability mass than those of a normal distribution.

Synthetic data are used in the analysis to calculate the corresponding option prices and to show how the option prices differ when the net issuance I_N changes. In addition, different volatility smiles are compared to the synthetic volatility smile with varying I_N.

4.2.2 Deribit options exchange

Deribit is the leading crypto asset options exchange in terms of volumes and significance. ETH option data was fetched from the Deribit API using Python 3. A JSON file containing detailed data on the options was received for the date 31 August 2023. The data was then parsed and structured into a format that was more suitable for analysis. The processed dataframe consists of ETH call options with varying strike and expiration times. The data consist of the previous 24 hours of the snapshot on 31 August 2023. The size of the dataframe is 14 columns, 214 rows, and its head is presented in Table 2 below.

	volume_usd	underlying_price	estimated_delivery_price	underlying_index	instrument_name	interest_rate
0	20.65	1716.25	1708.1	ETH-27OCT23	ETH-27OCT23-2400-C	0
1	50883.02	1708.05	1708.1	ETH-8SEP23	ETH-8SEP23-1750-C	0
2	7677.05	1707.82	1708.1	ETH-1SEP23	ETH-1SEP23-1450-C	0
5	0.00	1749.61	1708.1	ETH-29MAR24	ETH-29MAR24-200-C	0
10	41392.03	1731.17	1708.1	ETH-29DEC23	ETH-29DEC23-2200-C	0

creation_timestamp	base_currency	mark_price_usd	bid_price_usd	ask_price_usd	expiry_date	strike_price	time to expiry
2023-08-31 12:06:21	ETH	7.405619	7.036625	7.723125	2023-10-27	2400.0	0.156164
2023-08-31 12:06:21	ETH	13.862534	13.664400	14.518425	2023-09-08	1750.0	0.021918
2023-08-31 12:06:21	ETH	257.810799	239.948710	269.835560	2023-09-01	1450.0	0.002740
2023-08-31 12:06:21	ETH	1549.970751	1537.032385	1563.276535	2024-03-29	200.0	0.578082
2023-08-31 12:06:21	ETH	33.795901	32.892230	35.488985	2023-12-29	2200.0	0.328767

Table 2: Processed Python dataframe of the Deribit ETH call option data

The column name *volume_usd* refers to the 24h USD volume of the instrument given in the *instrument_name* column. All prices are denominated in USD in the dataframe. The *underlying_price* refers to the ETH spot price for the specific instrument. The spot prices may differ slightly due to bid-ask spreads and observation times. The *estimated_delivery_price* is consistently equal across various instruments, since it refers to the forward underlying price at expiration. All spot prices gravitate towards this same forward price. The columns *mark_price_usd*, *bid_price_usd*, and *ask_price_usd*

all refer to the call option market prices. The column *time_to_expiry* is the expiration time in years and is derived from the difference of *expiry_date* and *creation_timestamp*. This type of data formatting is sufficient for the purposes of analysis.

4.3 Analysis overview

The analysis of the data sets is focused on two main goals to answer the research questions. These goals are to understand how the net issuance changes in the BSM model affect option prices when volatility is known, and conversely, how these changes affect implied volatilities when option market prices are known. Furthermore, understanding how option expiration times affect these dynamics is analyzed.

It is straightforward to calculate the implied option prices with both versions of the BSM formula when there are predefined constant volatilities for each strike price. However, comparing implied volatilities with actual market prices from Deribit data requires numerical root-finding methods, because equation $C_{BSM} = C_{market}$ does not have analytic solutions for volatility. In the analysis, the bisection method is used due to its comparable benefits to other methods in this specific situation. The reasoning for this selection and the algorithm is presented in Section 4.3.1.

4.3.1 Numerical methods

There are many widely used numerical root finding algorithms in addition to the bisection method, such as Newton-Raphson or the secant method. The main logic for selecting the bisection method in this analysis is the interest in guaranteeing convergence in as many cases as possible, possibly at the cost of computational time. The data set cannot be considered large, and the computations are not intensive. Therefore, there is no point in optimizing computational efficiency at any trade-off cost. Newton-Raphson and the secant methods are more prone to the initial parameter selections, and root convergence depends on these initial parameter values. The bisection method is guaranteed to converge, if the function f is continuous on an interval $[a, b]$ such that $f(a)$ and $f(b)$ have opposite signs. The goal is to maximize the accuracy of each numerical estimate of implied volatility at each strike price. The bisection algorithm is presented below.

When estimating the traditional implied volatility, the function is defined as

$$f(\sigma) = C_{\text{BSM}}(S, K, T, r, \sigma) - C_{\text{market}}. \tag{54}$$

Here C_{BSM} is the BSM call option pricing formula and C_{market} is the market price of the option. The Bisection method consists of the following steps:

1. Choose the initial interval $[a, b]$ such that $f(a)f(b) < 0$. This indicates that the function $f(\sigma)$ changes sign in the interval.

2. Calculate the midpoint $c = {}^{(a+b)}/_{2}$.

3. Evaluate the function at the midpoint, $f(c)$.

4. If $f(c)$ is very close to zero (within a predefined tolerance), then c is the root of the function and the algorithm stops.

5. If $f(c)$ is not close to zero (not within a predefined tolerance), determine the subinterval where the root lies:

   - If $f(a)f(c) < 0$, then the root lies in the interval $[a, c]$, so set $b = c$.
   - If $f(b)f(c) < 0$, then the root lies in the interval $[c, b]$, so set $a = c$.

6. Repeat steps 2 to 5 until the root is found or the maximum number of iterations is reached.

When estimating the implied volatilities using the crypto BSM, the algorithm is the same except for the function definition, which is:

$$f(\sigma) = C_{\text{cryptoBSM}}(S, K, T, r, i, b, \sigma) - C_{\text{market}}, \tag{55}$$

which considers the continuous issuance rate and the continuous burn rate of the crypto asset, given by the Equations (43) - (46).

5 Results and analysis

This section presents the results of the model comparison analysis. In Section 5.1, synthetic data are used as a basis, while Deribit market data are used in Section 5.2. Section 5.3 summarizes the key insights from the results.

5.1 Model comparison with synthetic data

First, option prices corresponding to the synthetic volatility smile are calculated using a standard BSM model without dividends.

Figure 5: Call option prices for the synthetic data with strikes between 1200 and 2800. Time to expiration $t = 1$.

Figure 5 shows how the option prices are more valuable further in-the-money. In addition, option prices typically decrease asymptotically as the strike price increases after at-the-money price.

Next, call option prices are plotted with varying net issuance rates.

Figure 6: Call option prices for the synthetic data with different values for net issuance I_N, with strikes between 1800 and 2200. Time to expiration $t = 1$.

Figure 6 shows how the option market prices differ as the net issuance rate I_N changes. The center green graph corresponds to the graph in Figure 5. The blue top graph corresponds to the option prices with negative net issuance rates, resulting in higher option prices. The bottom violet graph corresponds to option prices with positive net issuance rates, resulting in lower option prices. Notably, the absolute price differences increase moving further in-the-money, and decrease for out-the-money strikes.

The effect of changing the option expiration time is in Figure 7.

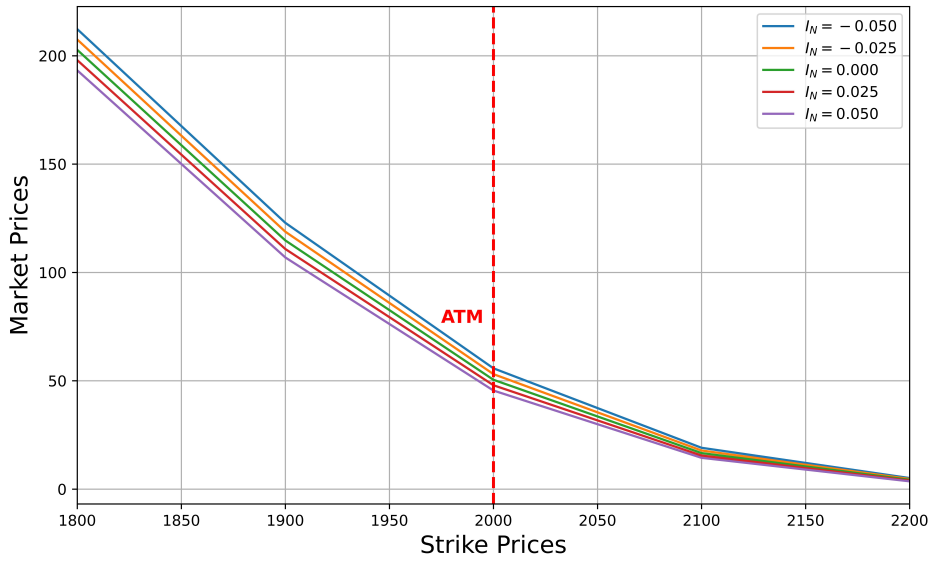

Figure 7: Call option prices impled by the synthetic data with different values for net issuance I_N, with strikes between 1800 and 2200. Time to expiration $t = 0.1$.

Figure 7 shows how the effect of changing net issuance rates decreases as option expiration time decreases. This is because the options have less time value.

We now have a basic theoretical understanding of how the call option prices behave under varying net issuance rates and option expiration time, and we move on to compare volatility structures.

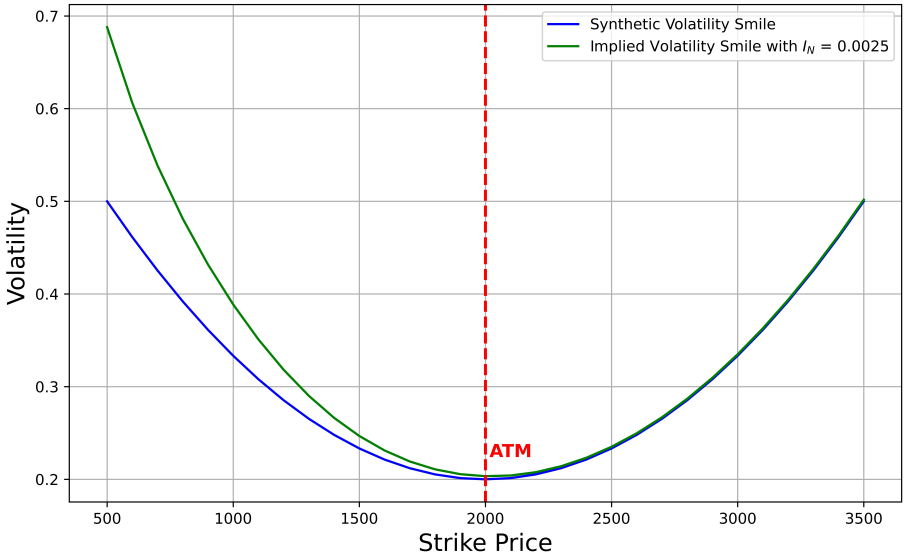

Figure 8: Volatility structure comparison with strikes between 500 and 3500. Net issuance $I_N = 0.0025$. Time to expiration $t = 1$.

Figure 8 compares the synthetic volatility smile to a smile corresponding to the crypto asset BSM implied volatilities with a low positive net issuance rate. As can be seen, the net issuance rate introduces skewness to the volatility structure, especially for in-the-money strikes. A low net issuance rate is used to properly compare to the different volatility structures. With higher net issuance rates, the deep-in-the-money implied volatilities increase aggressively, making the structures more difficult to compare. The volatility implied by the crypto asset BSM is higher everywhere with a positive net issuance rate. However, as the strike price increases, the implied volatilities approach each other with the two different models.

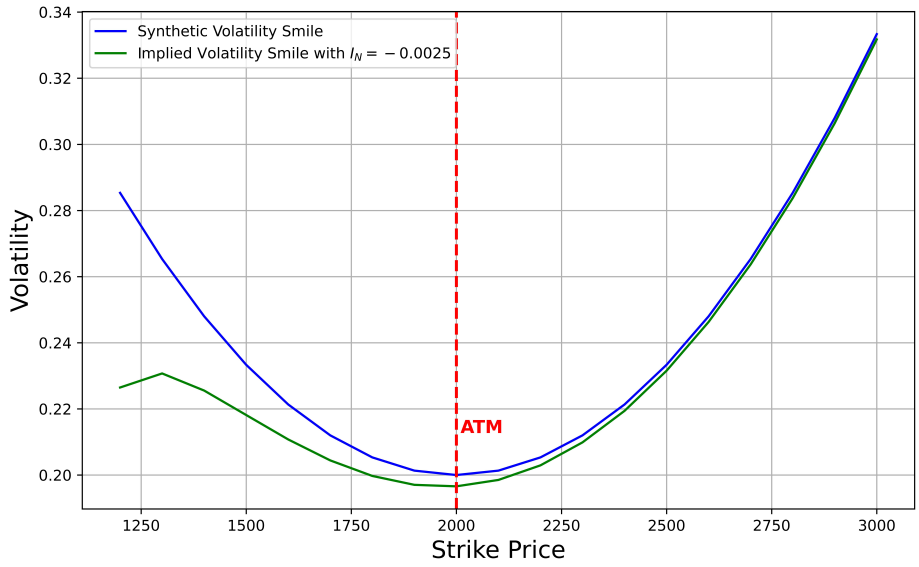

Figure 9: Volatility structure comparison with strikes between 1200 and 3500. Net issuance $I_N = -0.0025$. Time to expiration $t = 1$.

Figure 9 demonstrates the same skewness phenomenon as Figure 8, but for negative net issuance rates. Now, the volatilities implied by the crypto asset BSM are systematically lower everywhere and similarly approach each other as strike prices increase. A different strike interval is chosen such that the comparison is meaningful. Below 1200 strike prices, the crypto asset BSM implied volatilities start to aggressively trend down. This is in line with the behavior of Figure 8, where the implied volatilities increase, respectively.

We now have a basic theoretical understanding of how the call option prices and volatility structures behave with the traditional BSM and the crypto asset BSM with varying net issuance rates. In Section 5.2, the comparison is applied to Deribit options data.

5.2 Model comparison with Deribit data

First, an index of ETH options is chosen from Deribit and plotted against all available strike prices. The options are chosen to have an expiration time of approximately half a year, since the synthetic data mostly covered cases with expiration time of one year. Therefore, the results with synthetic data and real-world data should be roughly comparable. Moreover, half-year option expiration time ensures that the model is very accurate (note Section 4.1.3), but the changes in net issuance have a noticeable effect.

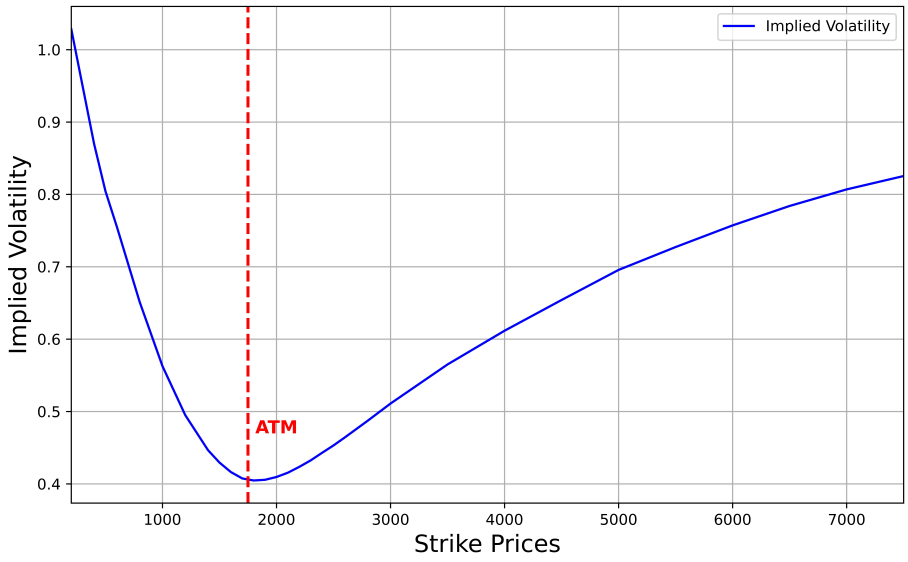

Figure 10: Volatility structure of the Deribit options index ETH-29MAR24 with all available strikes between 200 and 7000. Net issuance $I_N = 0.00$. Time to expiration $t = 0.578082$. Date: 31.08.2023.

Figure 10 shows the implied volatilities for the Deribit call option index "ETH-29MAR24" using a standard BSM approach. The shape of the plot is not a perfectly symmetric smile, which is natural for real-world options market data.

In Figure 11 below, the strike range is narrowed such that the implied volatilities form a smile more comparable to the synthetic volatility smile.

Figure 11: Volatility structure of the Deribit options index ETH-29MAR24 with strikes between 500 and 3500. Net issuance $I_N = 0.00$. Time to expiration $t = 0.578082$. Date: 31.08.2023.

Now, we can calculate the crypto asset BSM implied volatilities to the same graph for comparison with a non-zero net issuance rate.

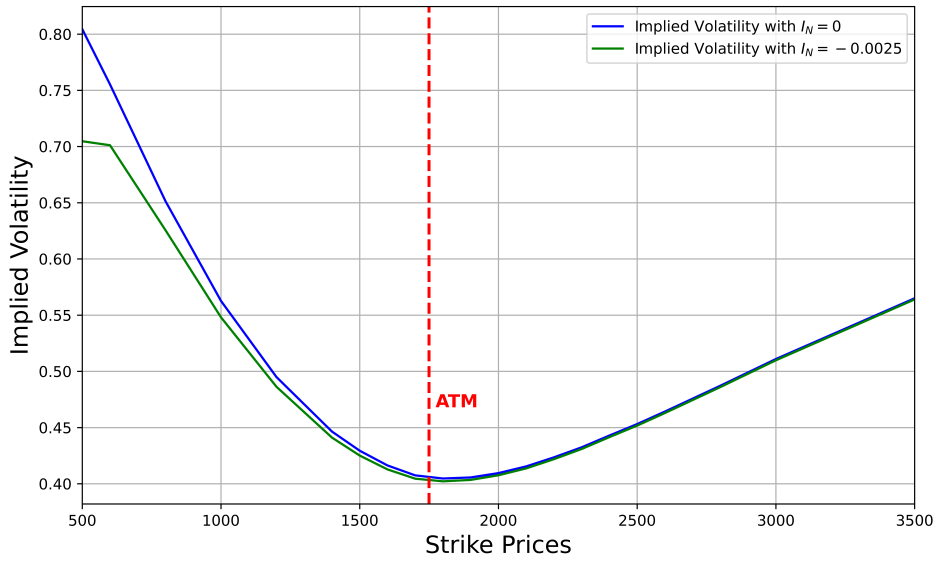

Figure 12: Volatility structure of the Deribit options index ETH-29MAR24 with strikes between 500 and 3500. Net issuance $I_N = -0.0025$. Time to expiration $t = 0.578082$. Date: 31.08.2023.

Figure 12 compares the implied volatilities of the traditional BSM and the crypto asset BSM with a low negative net issuance rate of −0.0025. This net issuance rate roughly corresponds to the net issuance of ETH during the last year [17]. Therefore, this comparison suggests that, according to the crypto asset BSM, the implied volatilities for ETH should be lower than currently considered, especially for deep-in-the-money calls.

Finally, the graph below demonstrates the hypothetical scenario in which the net ETH issuance rate decreases to −0.01, highlighting the most drastic differences in the volatility structure.

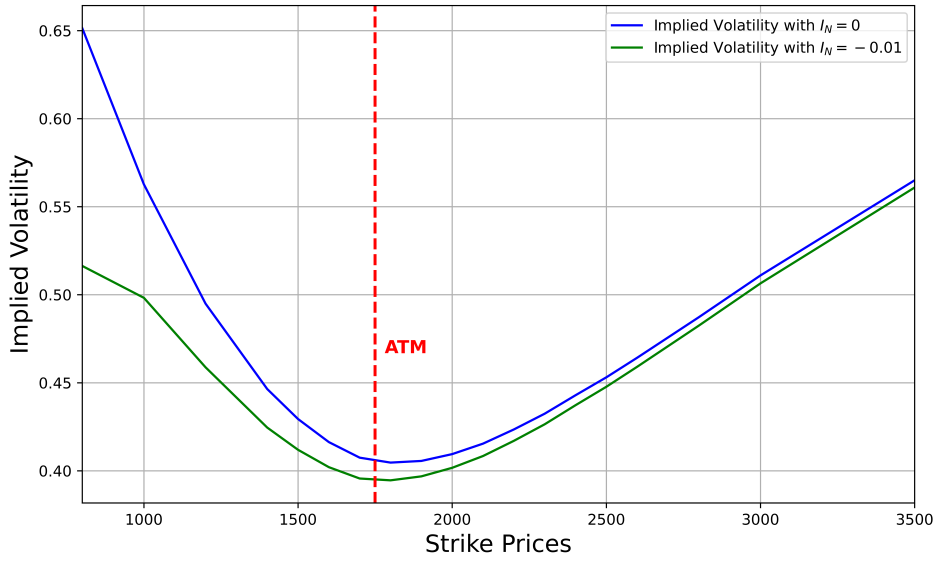

Figure 13: Volatility structure of the Deribit options index ETH-29MAR24 with strikes between 700 and 3500. Net issuance $I_N = -0.01$. Time to expiration $t = 0.578082$. Date: 31.08.2023.

Figure 13 shows how the implied volatility structures have considerably higher differences compared to the two models with a slightly more negative net issuance rate. Specifically, the difference for at-the-money price is significant compared to Figure 12.

5.3 Key findings

To summarize the key findings, call option prices increase for all strikes when the net issuance parameter is negative. Conversely, the prices decrease when the parameter is positive. When strike prices decrease, the absolute differences become larger. When strike prices increase significantly, option prices approach each other.

The net issuance rate introduces skewness in volatility structures. This skewness is weighted for deep-in-the-money options, which is consistent with the behavior of option prices. As strike prices increase significantly, the implied volatilities asymptotically approach each other.

Moreover, the sensitivity of the results to even minor changes in the net issuance rate parameter is noteworthy. Figures 12 - 13 demonstrate this effect. This indicates that the inclusion of the net issuance rate can cause significant changes in option pricing. Consequently, options could be fundamentally mispriced if the parameter is completely ignored.

The implied volatility graphs publicly available on the Deribit exchange are calculated without considering net issuance rates [50]. This can also be visually confirmed with the volatility structures calculated with the traditional BSM. Interestingly, the crypto asset BSM implied volatility structure for the Deribit options index ETH-29MAR24 forms a more symmetric smile on the chosen strike range. This can be coincidence or simply be explained by market expectations. However, it could also be explained by the market already understanding the significance of net issuance rates for crypto asset option pricing, and the crypto asset BSM implied volatility smile reflects this market knowledge. More analysis would be needed across various ETH options indices to conclude anything definitively.

6 Conclusions

6.1 Discussion

The main contribution of the thesis is the identification of a deterministic factor in the pricing of crypto asset options, the supply change rate, which is not taken into account in the traditional BSM model. The extended BSM model, or alternatively the crypto asset BSM, presented in this thesis includes this rate in the model. The supply change rate can take both positive and negative values within its mathematically defined limits. Moreover, the crypto asset BSM can be used for any other crypto asset that has a supply change parameter, preferably with low block times.

The first research question was to determine the impact that supply changes have on the BSM model when pricing ETH options. Section 4 mathematically formulates the impact by extending the BSM model to account for supply changes by introducing a net issuance rate variable to the equations. The second research question was about the comparison of the extended BSM model with the traditional approach to option pricing and implied volatility structures. The numerical results in Section 5 confirm that even minor changes in the net issuance rate cause meaningful changes in the option pricing and volatility structures. In particular, volatility structures experience an increasing skewness for deep-in-the-money call options.

The key limitiation in the thesis is the use of Taylor's approximation in the formulation of the crypto asset BSM. Therefore, the effects of the approximation are rigorously modeled and numerically studied. The accuracy of the crypto asset BSM decreases for long-expiration options with high net isuance rates. Consequently, the model is suitable for the majority of ETH options that are typically available in standard option exchanges. An obvious improvement and a motivation for further research is solving the crypto asset BSM analytically without the use of an approximation. This analytical version would be more suitable for the pricing of options across all expiration and net issuance rates.

Furthermore, another limitation is the assumption that the net issuance rate is constant in the crypto asset BSM. In reality, the net issuance rate can be stochastic with its own drift and volatility parameters. The crypto asset BSM could be extended to consider this in further research on the topic. In addition, the comparison analysis presented in Section 5 can be performed for different option products, which could strengthen the case for the theoretical and numerical results presented.

The BSM model is the most widely adapted options pricing model in financial markets. For this reason, it has already been extended to various financial instruments, including futures, bonds, and foreign currencies. This thesis extends the BSM to the nascent new asset class called crypto assets, and specifically to Ethereum, the second largest crypto asset.

The development of pricing models for new financial technologies is important for the general efficiency of the market. Crypto assets as a phenomenon are widely dismissed as something they are only partly: Internet currencies. Ethereum is a global decentralized protocol on top of which different types of new financial applications can be built. ETH is a unique financial asset that is a combination of a currency, a commodity, and a security. It is my sincere hope that this thesis plays a role not only in the improvement of crypto asset options valuations, but also in explaining what Ethereum is as a financial technology.

References

[1] Vitalik Buterin et al. A next-generation smart contract and decentralized application platform. *Ethereum whitepaper*, 3(37), 2014.

[2] Fischer Black and Myron Scholes. The pricing of options and corporate liabilities. *Journal of Political Economy*, 81(3):637–654, 1973.

[3] Mark S Grinblatt, Ronald W Masulis, and Sheridan Titman. The valuation effects of stock splits and stock dividends. *Journal of Financial Economics*, 13(4):461–490, 1984.

[4] Steven L Heston. A closed-form solution for options with stochastic volatility with applications to bond and currency options. *The Review of Financial Studies*, 6(2):327–343, 1993.

[5] Louis Bachelier. Théorie de la spéculation. In *Annales scientifiques de l'École normale supérieure*, volume 17, pages 21–86, 1900.

[6] Cloudflare. What is a protocol? https://www.cloudflare.com/learning/network-layer/what-is-a-protocol/, 2023. Accessed: 21/08/2023.

[7] Andreas M Antonopoulos and Gavin Wood. *Mastering Ethereum: Building Smart Contracts and Dapps*. O'Reilly Media, 2018.

[8] Chris Dannen. *Introducing Ethereum and Solidity*, volume 1. Springer, 2017.

[9] Ethereum average block time. https://ycharts.com/indicators/, 2023. Accessed: 23/08/2023.

[10] Chris Dixon. Why decentralization matters. https://onezero.medium.com/why-decentralization-matters-5e3f79f7638e, 2018. Accessed: 22/08/2023.

[11] Coingecko. https://www.coingecko.com/en/coins/ethereum. Accessed on 23rd Feb, 2023.

[12] Alan Mathison Turing et al. On computable numbers, with an application to the entscheidungsproblem. *Journal of Mathematics*, 58(345-363):5, 1936.

[13] Ethereum Foundation. Introduction to Ethereum. https://ethereum.org/en/developers/docs/intro-to-ethereum/, 2023. Accessed: 22/08/2023.

[14] Ethereum Foundation. The Merge. https://ethereum.org/en/roadmap/merge/, 2023. Accessed: 23/08/2023.

[15] Satoshi Nakamoto. Bitcoin whitepaper. *https://bitcoin.org/bitcoin.pdf*, 2008.

[16] Ethereum Foundation. Ethereum post-merge issuance. https://ethereum.org/en/roadmap/merge/issuance/, 2023. Accessed: 23/08/2023.

[17] Etherscan. Ethereum supply growth chart. https://etherscan.io/chart/ethersupplygrowth, 2023. Accessed: 23/08/2023.

[18] Token Terminal. Ethereum project overview. https://tokenterminal.com/terminal/projects/ethereum, 2023. Accessed: 23/08/2023.

[19] Collin Myers and Mara Schmiedt. The Internet Bond: Digital Work Agreements in the Web3.0 Era. August 2020.

[20] William Hinman. Digital asset transactions: When Howey met Gary (plastic). https://www.sec.gov/news/speech/speech-hinman-061418, 2018. Accessed: 23/08/2023.

[21] Nikhilesh De. CFTC chairman confirms Ether cryptocurrency is a commodity. https://www.coindesk.com/cftc-chairman-confirms-ether-cryptocurrency-is-a-commodity, 2019. Accessed: 23/08/2023.

[22] CoinDesk. SEC chairman Gensler suggests again that proof-of-stake tokens are securities: Report, March 2023. Accessed: 23/08/2023.

[23] U.S. Securities and Exchange Commission. SEC charges Coinbase for operating as an unregistered securities exchange, broker, and clearing agency. https://www.sec.gov/news/press-release/2023-102, 2023. Accessed: 23/08/2023.

[24] Kate Rooney. Coinbase is unlike any market debut Wall Street has ever seen. https://www.cnbc.com/2021/04/14/coinbase-is-unlike-any-market-debut-wall-street-has-ever-seen.html, April 2021. Accessed: 23/08/2023.

[25] European Parliament and Council of the European Union. Regulation (EU) 2023/1114 of the European Parliament and of the Council of 24 November 2023. https://eur-lex.europa.eu/legal-content/EN/TXT/?uri=CELEX%3A32023R1114, November 2023. Accessed: 23/08/2023.

[26] CoinGecko. Crypto derivatives market research. https://www.coingecko.com/research/publications/crypto-derivatives-market, 2023. Accessed: 24/08/2023.

[27] The Block. Crypto markets: Options. https://www.theblock.co/data/crypto-markets/options, 2023. Accessed: 24/08/2023.

[28] S Sapna and Biju R Mohan. Estimation of Implied Volatility for Ethereum Options Using Numerical Approximation Methods. *International Conference on Information Systems and Management Science*, 1:541–553, 2022.

[29] S Sapna and Biju R Mohan. Comparative Analysis of Root Finding Algorithms for Implied Volatility Estimation of Ethereum Options. *Computational Economics*, 2023.

[30] Ai Jun Hou, Weining Wang, Cathy YH Chen, and Wolfgang Karl Härdle. Pricing cryptocurrency options. *Journal of Financial Econometrics*, 18(2):250–279, 2020.

[31] Paolo Pagnottoni. Neural network models for bitcoin option pricing. *Frontiers in Artificial Intelligence*, 2:5, 2019.

[32] Kalle Kytölä. Probability Theory at Aalto University Department of Mathematics and Systems Analysis. https://math.aalto.fi/~kkytola/files_KK/lectures_files_KK/ProbaTh-2019.pdf, 2019.

[33] Rick Durrett. *Probability: Theory and Examples*, volume 49. Cambridge university press, 2019.

[34] Jean Jacod and Philip Protter. *Probability Essentials*. Springer Science & Business Media, 2004.

[35] David Williams. *Probability with Martingales*. Cambridge University Press, 1991.

[36] Ioannis Karatzas and Steven Shreve. *Brownian Motion and Stochastic Calculus*, volume 113. Springer Science & Business Media, 1991.

[37] Eveliina Peltola. Brownian motion, Martingales, and Stochastic Analysis at Aalto University Department of Mathematics and Systems Analysis. https://mycourses.aalto.fi/pluginfile.php/1768438/course/section/222709/BM_and_stoch_anal.pdf, 2023.

[38] Ruth Kaila. *The Integrated Volatility Implied by Option Prices, a Bayesian Approach*. Teknillinen korkeakoulu, 2008.

[39] Sheldon M Ross. *Stochastic Processes*. John Wiley & Sons, 1995.

[40] Emanuel Parzen. *Stochastic Processes*. Society for Industrial and Applied Mathematics, 1999.

[41] Bernt Oksendal. *Stochastic Differential Equations: An Introduction with Applications*. Springer Science & Business Media, 2013.

[42] Jean-François Le Gall. *Brownian motion, Martingales, and Stochastic Calculus*. Springer, 2016.

[43] Kiyosi Itô. Stochastic Integral. *Proceedings of the Imperial Academy*, 20(8):519–524, 1944.

[44] Paul Wilmott. *Paul Wilmott introduces Quantitative Finance*. John Wiley & Sons, 2007.

[45] Paul Wilmott. *Paul Wilmott on Quantitative Finance*. John Wiley & Sons, 2013.

[46] Martin Baxter and Andrew Rennie. *Financial Calculus: An Introduction to Derivative Pricing*. Cambridge University Press, 1996.

[47] Fabrice Douglas Rouah. Four derivations of the Black-Scholes formula. https://www.frouah.com/, 2023. Accessed: 23/08/2023.

[48] Robert C Merton. Theory of rational option pricing. *The Bell Journal of Economics and Management Science*, 4(1):141–183, 1973.

[49] Robert C Merton and Paul Anthony Samuelson. *Continuous-Time Finance*. Blackwell Boston, 1992.

[50] Deribit Ethereum options contract specification. https://www.deribit.com/kb/options, 2023. Accessed: 28/09/2023.